Gastroenterology 2015;149:886–889

BRIEF REPORTS

Exome Sequencing Reveals Germline *SMAD9* Mutation That Reduces Phosphatase and Tensin Homolog Expression and Is Associated With Hamartomatous Polyposis and Gastrointestinal Ganglioneuromas

Joanne Ngeow,[1,2,3,4] Wanfeng Yu,[1,2] Lamis Yehia,[1,2] Farshad Niazi,[1,2] Jinlian Chen,[1,2] Xuhua Tang,[5] Brandie Heald,[1,2,6] Junying Lei,[1,2] Todd Romigh,[1,2] Lisa Tucker-Kellogg,[7] Kiat Hon Lim,[8] Haiwei Song,[5] and Charis Eng[1,2,6,9,10]

[1]*Genomic Medicine Institute, Cleveland Clinic, Cleveland, Ohio;* [2]*Lerner Research Institute, Cleveland Clinic, Cleveland, Ohio;* [3]*Division of Medical Oncology, National Cancer Centre, Singapore;* [4]*Oncology Academic Clinical Program, Duke-NUS Graduate Medical School, Singapore;* [5]*Institute of Molecular and Cell Biology, A*STAR, Singapore;* [6]*Taussig Cancer Institute, Cleveland Clinic, Cleveland, Ohio;* [7]*Centre for Computational Biology, Duke-NUS Graduate Medical School, Singapore;* [8]*Department of Pathology, Singapore General Hospital, Singapore;* [9]*CASE Comprehensive Cancer Center, Case Western Reserve University, Cleveland, Ohio; and* [10]*Department of Genetics and Genome Sciences, Case Western Reserve University, Cleveland, Ohio*

Hamartomatous polyposis syndromes (HPS) account for a small but appreciable proportion of inherited gastrointestinal cancer predisposition syndromes; patients with HPS have an increased risk for colon and extracolonic malignancies. We present a unique case of familial juvenile polyposis syndrome associated with gastrointestinal ganglioneuromas of unknown etiology. The patient was tested for HPS-associated genes, but no mutation was detected. Exome sequencing identified a germline heterozygous mutation in *SMAD9* (*SMAD9*^{V90M}). This mutation was predicted to be an activating mutation. HEK cells transfected to express SMAD9^{V90M} had reduced expression of phosphatase and tensin homolog; this reduction was also observed in a polyp from the patient. We have therefore identified a new susceptibility locus for HPS. Patients with hamartomatous polyposis in the colon associated with ganglioneuromatosis should be referred for genetic assessments.

Keywords: Hamartomatous Polyps; Ganglioneuromas; Colorectal Cancer; SMAD Signaling.

Six distinct autosomal-dominant inherited hamartomatous polyposis syndromes (HPS) have been described (Supplementary Table 1). It is now known that many of these syndromes carry a substantial risk for developing colonic and extracolonic malignancies, depending on which gene(s) are involved. Clinical management is informed by the specific gene.

It is important to note that a significant number of patients have no family history. Therefore, the diagnosis of these syndromes remains a clinical process primarily. These important, potentially heritable, polyp conditions are a challenge for clinicians because individuals present with features that overlap one or more of the syndromes.

We describe here a novel hamartomatous polyposis susceptibility gene discovered while investigating a 38-year-old white man with HPS, presenting with diarrhea and weight loss, because of the persistence of his symptoms. Colonoscopy revealed diffuse 3- to 5-mm polyps in his ascending, transverse, descending, and sigmoid colon. Thirty of these were removed, and reported as showing hamartomatous polyps admixed with either mature adipose or ganglioneuromatous proliferation. Two ascending colon polyps blocks was re-reviewed by our gastrointestinal pathologist and confirmed as ganglioneuromatous polyps (Figure 1*A*). Upper endoscopy was unremarkable.

His family history is significant; his father had diffuse polyposis and died in his 40s; the patient did not know the cause of death. His paternal uncle and aunt died from early-onset colorectal cancer in their 40s (Figure 1*B*). The genetic differential diagnosis for gastrointestinal ganglioneuromas includes Cowden syndrome[1,2] (CS), multiple endocrine neoplasia type 2B, and type I neurofibromatosis (Supplementary Table 1). Because physical examination did not reveal the stigmata of multiple endocrine neoplasia type 2B or type I neurofibromatosis, CS was considered. He had no other CS-related individual features, such as macrocephaly, mucocutaneous manifestations, or personal history of cancer. Histologically, he did not present with characteristic juvenile polyps or Peutz-Jehgers polyps. This patient therefore did not fulfill clinical testing criteria for HPS and was instead enrolled in a prospective research study for HPS. He underwent sequencing and deletion/duplication analysis for *BMRP1A, SMAD4, phosphatase and tensin*

Abbreviations used in this paper: **BMP, bone morphogenetic protein; CS, Cowden syndrome; HPS, hamartomatous polyposis syndromes; JPS, juvenile polyposis syndrome; miR21, microRNA 21; mRNA, messenger RNA; PTEN, phosphatase and tensin homolog; WT, wild type.**

Most current article

0016-5085/$36.00
http://dx.doi.org/10.1053/j.gastro.2015.06.027

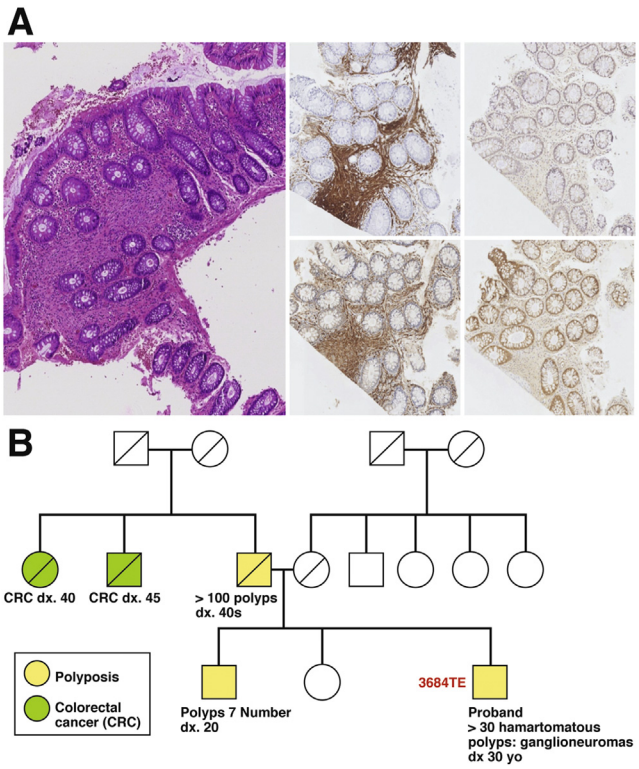

Figure 1. (*A*) Histological features (at 100× magnification). Clockwise from *top left*: (*i*) H&E stains showing spindle and polygonal nerve and ganglion cells; (*ii*) S100 stain highlights the lesional neural fibers; (*iii*) decreased PTEN expression; (*iv*) strongly positive p-ERK expression; and (*v*) decreased p-AKT expression. Bar = 100 μm. (*B*) Pedigree of proband-3684TE family.

homolog (*PTEN*), and *STK11*[1] but was mutation negative for these known HPS genes.

Because this was an unique case of familial HPS associated with gastrointestinal ganglioneuromas and colorectal cancer of unknown etiology, we hypothesized that functionally important sequences in either the PTEN or transforming growth factor−β/bone morphogenetic protein (BMP) signaling pathways might be affected and proceeded with whole exome sequencing (see Supplementary Materials and Methods).

We analyzed all sequence data for the presence of nonsense, frameshift, consensus splice site, and missense mutations after whole exome sequencing. Given the very unique histologic phenotype of the polyps seen in our patient, we focused our attention on mutations that were likely to be of biological importance, namely those in the canonical HPS signaling pathways (Supplementary Table 1). In this manner, we identified in our patient a novel germline heterozygous *SMAD9* V90M ($SMAD9^{V90M}$) missense mutation (Supplementary Figure 1*A*).

Structural modeling predicts $SMAD9^{V90M}$ as an activating mutation. The modeled SMAD8 (protein encoded by *SMAD9*) MH1 shows a globular fold containing 5 α-helices and 6 β-strands, where Val90 lies in the α4-helix. The MH1 domains of these SMADs recognize DNA through a β-hairpin made up of β2 and β3. Val90 is located in close proximity with the DNA binding interface and contacts residues Leu87 and His104 through hydrophobic interactions. Mutation of Val90 to a methionine would therefore cause the long side chain of methionine to clash with the neighboring His104. To relieve this steric clash, His104 would move toward the DNA phosphate backbone, therefore, enhancing the DNA binding of SMAD8 (Supplementary Figure 1*B*).

Functionally, we saw evidence to support $SMAD9^{V90M}$ as a gain-of-function mutation. We saw increased phosphorylation of SMAD9 in Flag-tagged $SMAD9^{V90M}$ transfected cells as compared with Flag-tagged *SMAD9* wild-type (WT) ($SMAD9^{WT}$) transfected HEK293 cells (Figure 2*A*). We observed increased inhibitor of differentiation 1 messenger RNA (mRNA) level in $SMAD9^{WT}$-transfected HEK cells with BMP4 stimulation (Figure 2*B*) with a greater increase in inhibitor of differentiation 1 expression in $SMAD9^{V90M}$-transfected HEK cells compared with that in $SMAD9^{WT}$ transfected cells. Interestingly, we observed that both protein (Supplementary Figure 1*C*) and mRNA levels (Figure 2*C*) of PTEN in lymphoblastoid cell lines derived from our patient were lower compared with lymphoblastoid cell lines from healthy participants, suggesting that $SMAD9^{V90M}$ mutation affects PTEN expression. Corroborating the lymphoblastoid cell line observations, reduced PTEN protein expression was evident in the patient's polyp (Figure 1*A*).

To functionally understand this observation, we transfected Flag-tagged $SMAD9^{WT}$ or Flag-tagged $SMAD9^{V90M}$ into HEK293 cells. Consistently, in $SMAD9^{V90M}$-transfected HEK293 cells, PTEN protein levels were significantly decreased compared with that in $SMAD9^{WT}$ cells (Figure 2*A*). Additionally, quantitative reverse transcription polymerase chain reaction for PTEN transcript in transfected cells showed lower PTEN mRNA level in $SMAD9^{V90M}$ cells compared with that in $SMAD9^{WT}$ cells (Figure 2*D*). However, SMAD9 was unable to directly bind the *PTEN* promoter, suggesting that it is not acting as a transcription factor (Supplementary Figure 1*D*). We then turned our attention to a direct downstream effector of BMP-SMAD9 signaling pathway, microRNA 21 (miR21), which has been shown to target PTEN directly and suppress PTEN expression.[3] We showed that miR21 expression level was increased significantly in BMP4-treated $SMAD9^{V90M}$-transfected cells compared with $SMAD9^{WT}$-transfected cells (Figure 2*E*) due to increased binding of $SMAD9^{V90M}$ to pri-miR21 (Supplementary Figure 2*C*) with consequent increased processing of pri-miR21 into mature miR21. We surmise, therefore, that $SMAD9^{V90M}$ is a gain-of-function mutation leading to increased miR21 expression, with consequent decreased PTEN stability at both mRNA and protein levels.

We subsequently screened 40 juvenile polyposis syndrome (JPS) patients and 40 CS patients with HPS who were mutation negative for *BMPR1A, STK11, SMAD4,* and *PTEN* for *SMAD9* mutations but did not detect any with *SMAD9* mutations. *BMPR1A* and *SMAD4* germline mutations account for 40%−45% of patients who meet criteria for JPS, in contrast, this *SMAD9* mutation is likely to be a private mutation, as we did not find a mutation in *SMAD9* outside of

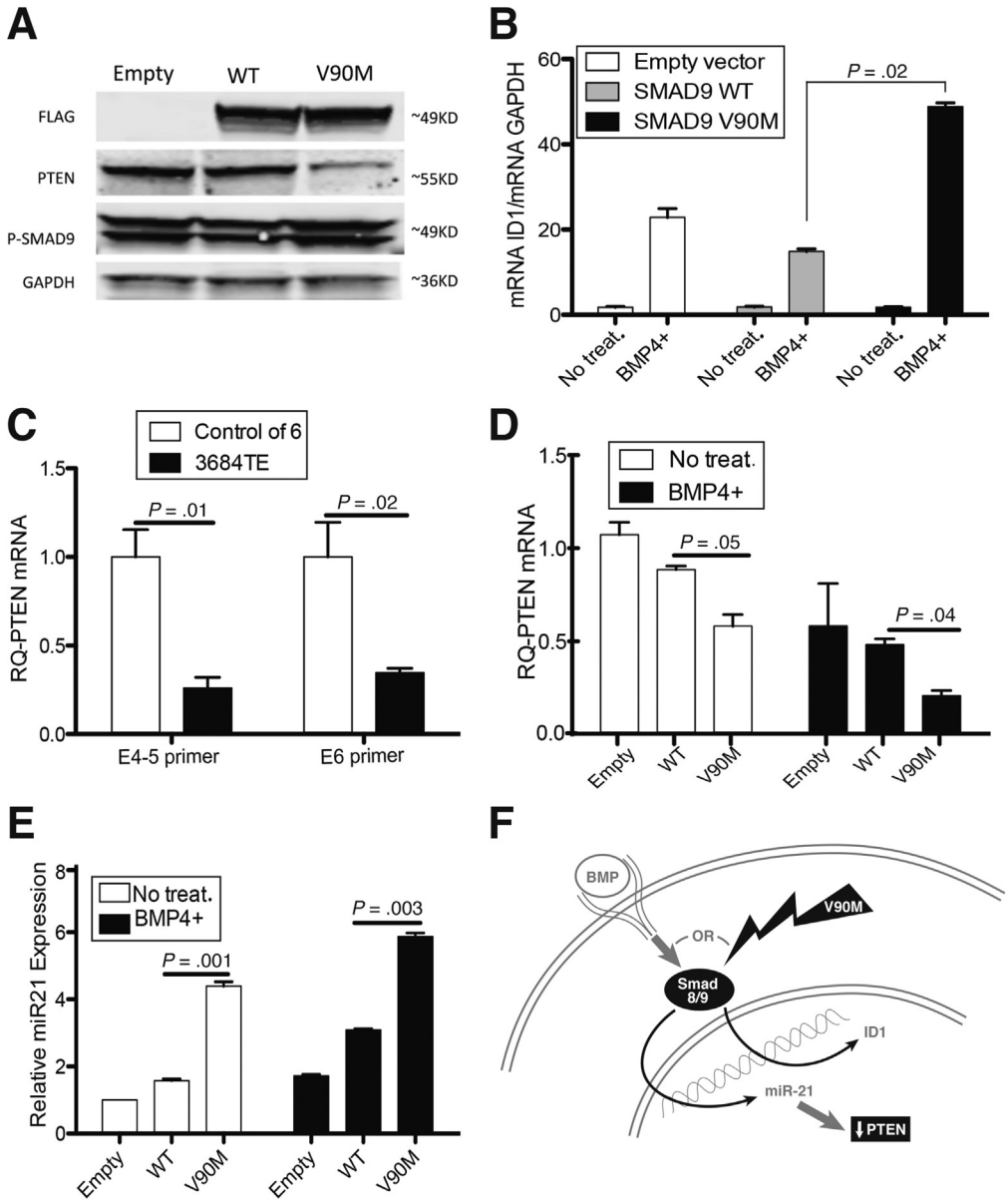

Figure 2. Gain-of-function *SMAD9*^{V90M} results in increased miR21 expression and reduced PTEN expression. (*A*) *SMAD9*^{V90M}-transfected cells show more phosphorylated-SMAD9 (P-SMAD9 row) and decreased PTEN protein expression (PTEN row) than cells transfected with *SMAD9*^{WT}. Note equal expression of WT SMAD9 and mutant SMAD9 (FLAG row). (*B*) *SMAD9*^{V90M} induces inhibitor of differentiation 1 (ID1) mRNA expression in BMP4-treated compared with sham-treated (No treat.) HEK293 cells. (*C*) PTEN mRNA levels (*bottom panel*) are significantly lower in our patient (3864TE)-derived lymphoblastoid cell lines compared with healthy controls. (*D*) PTEN mRNA expression in *SMAD9*^{V90M}-transfected cells was significantly lower than *SMAD9*^{WT}-transfected cells with (BMP4+) or without BMP4 (No treat.) stimulation. (*E*) *SMAD9*^{V90M}-transfected cells showed higher miR21 expression compared with *SMAD9*^{WT}-tranfected cells in the presence (BMP4+) or absence (No treat.) of BMP4. (*F*) *Schematic diagram* depicting the effect of *SMAD9*^{V90M} on ID1, miR-21, and PTEN expression. Also see text and Supplementary Figure 2*C*.

this family in limited subsets of patients with JPS or CS. Our patient, in addition to JPS, had significant ganglioneuromatosis, which is rare but overrepresented in CS patients with germline *PTEN* mutations.[1,2] We believe that our patient's *SMAD9* mutation results in gain-of-function in SMAD8, leading to reduced PTEN mRNA and protein stability, together, yielding a phenotype (ganglioneuromatous polyps) seen more commonly in patients with germline *PTEN* mutations. Our study suggests that this might be indirectly regulated by increased miR21expression (Figure 2*F*) secondary to increased binding of mutant-SMAD8 to pri-miR21, resulting in increased miR21 biogenesis, the latter consistent with Hata's demonstration that SMAD proteins controlling DROSHA-mediated maturation of miRs.[4] Our findings will need to be confirmed by future studies to fully understand the complex interactions between SMAD and PTEN signaling. Our study is limited by the unavailability of family members (either deceased or not

contactable) for segregation analysis despite multiple and prolonged attempts to do so.

We do, however, recommend that all patients with a clinical presentation of hamartomatous polyposis, especially those with gastrointestinal ganglioneuromas, be referred for genetic evaluation. It is worth highlighting that use of custom-gene panels relies on known susceptibility genes and will miss novel genes such as this. For select patients, subsequent clinical exome sequencing can prove fruitful.

Supplementary Material

Note: To access the supplementary material accompanying this article, visit the online version of *Gastroenterology* at www.gastrojournal.org, and at http://dx.doi.org/10.1053/j.gastro.2015.06.027.

References

1. **Ngeow J, Heald B**, et al. Gastroenterology 2013;144:1402–1409, 9 e1–5.
2. Heald B, et al. Gastroenterology 2010;139:1927–1933.
3. Drake KM, et al. Am J Respir Crit Care Med 2011;184:1400–1408.
4. Davis BN, et al. Nature 2008;454:56–61.

Author names in bold designate shared co-first authorship.

Received December 20, 2014. Accepted June 20, 2015.

Reprint requests
Address requests for reprints to: Charis Eng, MD, PhD, Genomic Medicine Institute, Cleveland Clinic, 9500 Euclid Avenue, NE-50, Cleveland, Ohio 44195. e-mail: engc@ccf.org; fax: (216) 636-0655.

Acknowledgments
Joanne Ngeow was an Ambrose Monell Cancer Genomic Medicine Fellow at the Cleveland Clinic Genomic Medicine Institute. Lamis Yehia is an International Fulbright Science and Technology Doctoral Fellow at the Cleveland Clinic Genomic Medicine Institute. Charis Eng is the Sondra J. and Stephen R. Hardis Chair of Cancer Genomic Medicine at the Cleveland Clinic and is an American Cancer Society Clinical Research Professor. The authors thank all our research participants and their clinicians who contributed to this study, the Genomic Medicine Biorepository of the Cleveland Clinic Genomic Medicine Institute, and our database and clinical research coordination teams for their meticulous up keeping and auditing of the clinical databases.

We thank Drs M. Aldred and K. Drake from the Genomic Medicine Institute for helpful discussions and *SMAD9* primers.

Conflicts of interest
The authors disclose no conflicts.

Supplementary Materials and Methods

Whole Exome Sequencing

Genomic DNA was extracted from blood. Exome enrichment was performed using the TruSeq SBS version 3 chemistry kit (Illumina Inc, San Diego, CA), followed by 100-bp paired-end sequencing using an Illumina HiSeq 2000 platform. Sequencing was performed at an Illumina Sequencing Service Center (Illumina Inc) in 8 lanes with 34 GB of data generated per lane. The mean sequence coverage was 80×, with >90% of the targeted regions covered by at least 10 reads for each exome. Sequencing data were analyzed and annotated by an in-house optimized pipeline. Raw sequencing reads were mapped to the human reference haploid genome sequence (Genome Reference Consortium human genome build 37, hg19) using the Burrows-Wheeler Aligner (BWA version 0.6.1).[1] Indel realignment, base and quality score recalibrations, and removal of polymerase chain reaction (PCR) duplicates from the resultant Binary Alignment Map files were done using the Genome Analysis Toolkit,[2,3] Sequence Alignment/Map (SAMtools), and Picard.[4] Variant discovery and genotype calling of single nucleotide variations and short insertions and deletions (indels, <50 bp) was performed using the Haplotype Caller of the Genome Analysis Toolkit.

Variant Filtration and Annotation

To prioritize causal variants, we applied the Annovar Variants Reduction pipeline.[5] First, we discarded synonymous variants and intronic variants >2 bp from exon boundaries. We retained variants in conserved genomic regions based on a 46-species alignment and removed variants existing in segmental duplication regions. We excluded variants that were observed in the 1000 Genomes Project (April 2012 release) or the NHLBI-ESP6500 exomes with a minor allele frequency >0.0005 and variants reported in dbSNP137 nonflagged database (excluding clinically associated SNPs). To predict the potential impact of missense variants on protein function, we used SIFT[6] with a cut-off score of 0.05 and PolyPhen2[7] with cut-off scores of 0.447 (HumanVar database) and 0.453 (HumanDiv database) to retain predicted deleterious variants. We also used CONsensus DELeteriousness (Condel),[8] which combines multiple prediction software algorithms (SIFT, PolyPhen2, and MutationAssessor[9]) into a single weighted score. All resultant variants were manually inspected through the Integrated Genomics Viewer (IGV, Broad Institute). We also used an in-house database containing variants from 20 exomes from pediatric subjects and 37 CS probands with unrelated phenotypes, sequenced with our patient cohort as an additional internal control filter. We excluded variants that appeared more than once in this in-house exome database. Mutations in candidate genes of interest were validated using PCR-based region-specific mutation analysis through Sanger sequencing.

Structural Biology

To predict the potential structural change caused by the *SMAD9*^{V90M} missense mutation, homology modeling was performed using SWISS-MODEL.[10,11] SMAD9 has 2 isoforms and is confusingly referred to as SMAD8, and so, we refer to it here as SMAD8/9. To verify the role of this residue in DNA binding, the SMAD8/9 MH1 model was superimposed with the structures of SMADs 1, 3, and 4 in complex with their respective cognate SMAD-binding element DNA via Dalilite server.[12]

RNA Extraction and Phosphatase and Tensin Homolog Quantitative Reverse Transcription Polymerase Chain Reaction

Total RNA was extracted from peripheral blood derived lymphoblastoid cell lines from controls and patients using GeneJET RNA Purification Kit (Thermo Scientific, Waltham, MA) according to the manufacturer's protocol, and subsequently treated with DNase I (Invitrogen, Carlsbad, CA). DNase treated total RNA was reverse-transcribed into complementary DNA using Superscipt III first-strand synthesis system for reverse transcription PCR (Invitrogen), as specified by the manufacturer. Quantitative PCR was performed on 7500 Real time PCR System (AB Applied Biosystems, 850 Lincoln Center drive, Foster City, CA) using the PTEN mRNA specific TaqMan primer-probe, PTEN exon 6−specific TaqMan primer-probe and Actin-β mRNA-specific TaqMan primer probe as endogenous loading control. PTEN mRNA specific primers and probe sequences: forward: 5′-AAGA CATTATGACACCGCCAAA-3′, reverse: 5′-GTGGGTTATGGTC TTCAAAAGGA-3′, probe: 6FAM-TTAATTGCAGAGTTGCA CAAT-MGBNFQ. PTEN exon6 specific primers and probe sequences: forward: 5′-CAGTCAGAGGCGCTATGTGTATTATT-3′, reverse: 5′- CAAACATCATCTTGTGAAACAACAGT-3′, probe: 6FAM-TACCTGTTAAAGAATCATCTGGATT-MGBNFQ. Actin-β mRNA specific primers and probe sequences: forward 5′- CTGGCACCCAGCACAATG-3′, reverse: 5′- CCGATC CACACGGAGTACTTG-3′, probe: VIC-AGATCAAGATCATTGCT CCT-MGBNFQ.

Phosphatase and Tensin Homolog Protein Analysis

HEK293 cells were plated 70% confluent in 6-well plates the day before transfection. Flag tagged *SMAD9* ^{WT}, *SMAD9* ^{V90M} plasmids or empty vector were transfected in HEK293 cells with transfection reagent Lipofectamine 3000 (Invitrogen, Grand Island, NY) according to manufacturer's provided protocol. Forty-eight hours post transfection, cells were treated with MG132 for 8 hours, or cycloheximide for 24 hours, respectively. Cells were then harvested and lysed with M-PER mammalian protein extraction reagent (Thermo Fisher Scientific Inc, Rockford, IL). Western blots were run with the lysates and blotted for anti-PTEN, anti−glyceraldehyde-3-phosphate dehydrogenase and anti-Flag antibodies.

Inhibitor of Differentiation 1 Quantitative Reverse Transcription Polymerase Chain Reaction

Total RNA were extracted from Flag tagged $SMAD9^{WT}$, $SMAD9^{V90M}$ plasmids or empty vector transfected HECK293 cells 48 hours post transfection. Reverse transcription was processed using Superscipt III first-strand synthesis system for reverse transcription PCR (Invitrogen). Inhibitor of differentiation 1 mRNA expression level was measured using quantitative PCR with inhibitor of differentiation 1−specific primers kindly provided by Dr Aldred's laboratory (Genomic Medicine Institute, Cleveland Clinic).

Chromatin Immunoprecipitation

To investigate if V90M mutation in *SMAD9* influences its function, firstly, we examined phosphorylation of SMAD9. We transfected Flag-tagged $SMAD9^{WT}$or Flag-tagged $SMAD9^{V90M}$ mutant into HEK293 cells. HEK293 cells were plated 70% confluent in 6-well plates the day before transfection. Flag-tagged $SMAD9^{WT}$, $SMAD9^{V90M}$ plasmid or empty vector, were transfected in in the cells with Lipofectamine 3000 (Invitrogen) according to manufacturer's provided protocol. Forty-eight hours post transfection, half of the transfected cells were treated with 8 nM BMP4 for 2 hours. Cells were processed for chromatin immunoprecipitation using Flag antibody (Sigma-Aldrich) and analyzed for PTEN promoter binding ability according to manual (EZ-ChIPTM Chromatin Immunoprecipitation Kit, EMD Millipore Corporation, Billerica, MA).

MicroRNA 21 Expression

Using $SMAD9^{WT}$and $SMAD^{V90M}$ plasmid transfected HEK293 cells, total RNA, including miRNA, were extracted from miRNeasy Mini Kit (Qiagen, Hilden, Germany). Complementary DNA synthesis was performed with TaqMan MicroRNA Reverse Transcription Kit with RT primer specific to miR21 or miRNU66 (TaqMan Small RNA Assay for miR21, TaqMan Small RNA Assay for miRNU66 and TaqMan Universal Master Mix II). miR21 and miRNU66 were amplified for 40 cycles in a 20-μL reaction. miR21 expression levels were analyzed using miRNU66 as internal control.

Pri-Micro RNA21 Reverse Transcription Polymerase Chain Reaction Followed by FLAG Immunoprecipitation in SMAD9-transfected HEK293 Cells

HEK293 cells were plated 70% confluent in 6-well plates the day before transfection. Flag-tagged $SMAD9^{WT}$, $SMAD9^{V90M}$ plasmid or empty vector, were transfected in in the cells with Lipofectamine 3000 (Invitrogen) according to manufacturer's provided protocol. Forty-eight hours post transfection, cell lysates were exacted and processed for FLAG immunoprecipitation using Flag antibody (Sigma-Aldrich). After centrifuging down Protein A/G plus agarose beads (Santa Cruz Biotechnology, Inc., Heidelberg, Germany), total RNA was extracted with miRNeasy Mini kit (Qiagen) for reverse transcription with SuperScript III First-Strand kit (Invitrogen). Probe for Pri-miR21 quantitative PCR was provided from TaqMan Pri-miRNA (has-mir-21) Assay kit (Applied Biosystems by Life Technologies, Carlsbad, CA). Pri-miR21 quantitative PCR was amplified for 40 cycles in a 20-μL reaction with triplicates.

References

1. Li H, et al. Bioinformatics 2009;25:1754–1760.
2. McKenna A, et al. Genome Res 2010;20:1297–1303.
3. DePristo MA, et al. Nat Genet 2011;43:491–498.
4. Li H, et al. Bioinformatics 2009;25:2078–2079.
5. Wang K, et al. Nucleic Acids Res 2010;38:e164.
6. Ng PC, et al. Nucleic Acids Res 2003;31:3812–3814.
7. Adzhubei IA, et al. Nat Methods 2010;7:248–249.
8. Gonzalez-Perez A, et al. Am J Hum Genet 2011;88:440–449.
9. Reva B, et al. Nucleic Acids Res 2011;39:e118.
10. Schwede T, et al. Nucleic Acids Res 2003;31:3381–3385.
11. Guex N, et al. Electrophoresis 1997;18:2714–2723.
12. Holm L, et al. Bioinformatics 2000;16:566–567.

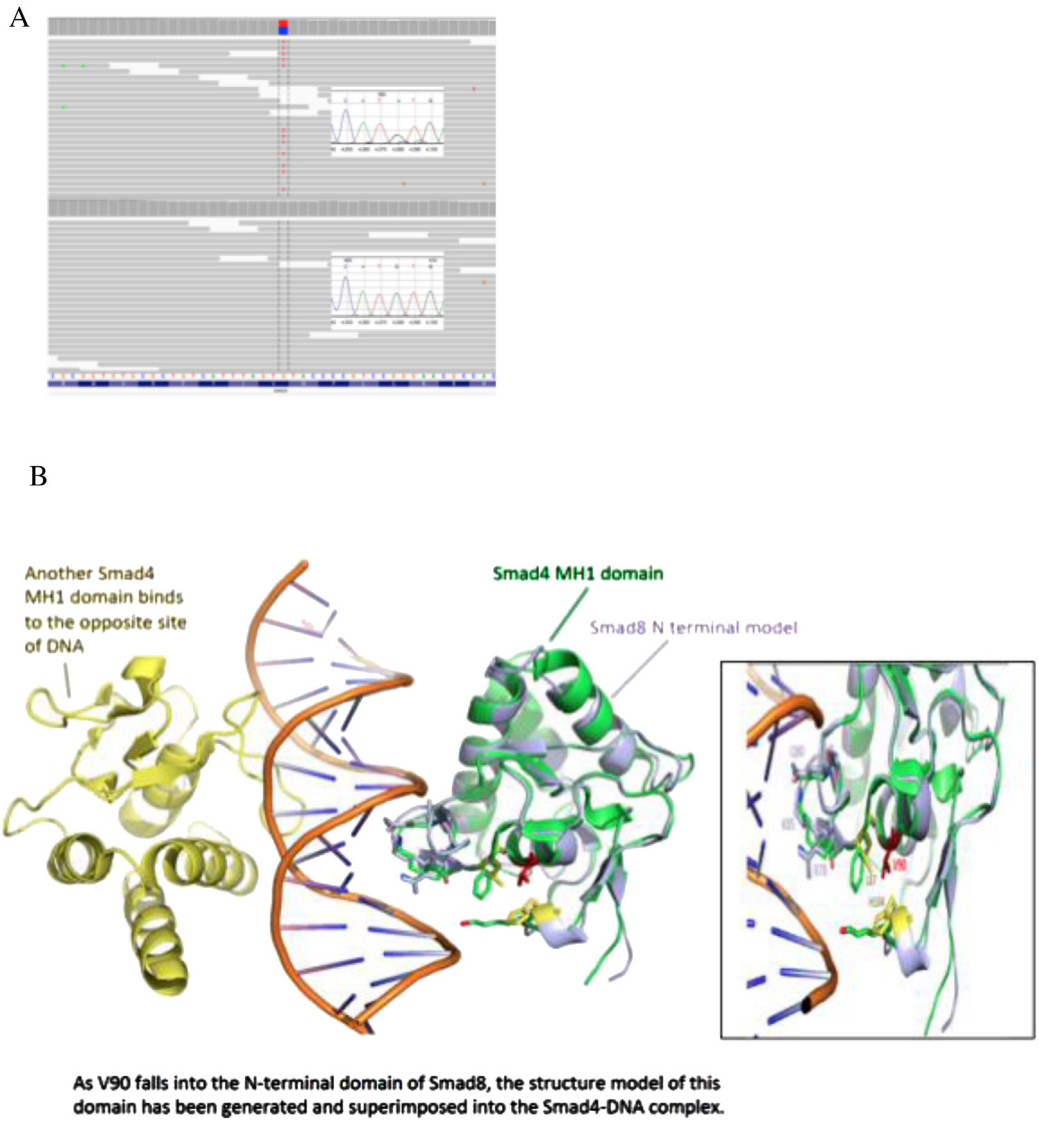

Supplementary Figure 1. (*A*) *SMAD9* V90M mutation. The *top panel* shows the Integrated Genome Viewer and Sanger sequencing results for the patient showing the heterozygous V90M mutation. The *lower panel* is the results from one of the internal controls used in this study showing the corresponding wild-type sequence. (*B*) Possible functional impact of V90M. The modeled SMAD8/9 MH1 shows a globular fold containing 5 α-helices and 6 β-strands, where Val90 lies in the α4-helix. Three residues in SMAD4 (equivalent to R78, Q80, and K85 in SMAD8) are the key residues that are involved in DNA interaction. Those residues are conserved in SMAD4 and SMAD8. Mutation of Val90 to a methionine would cause the long side chain of methionine to clash with the neighboring His104. To relieve this steric clash, His104 would move toward the DNA phosphate backbone, therefore, enhancing the DNA binding of SMAD 8.

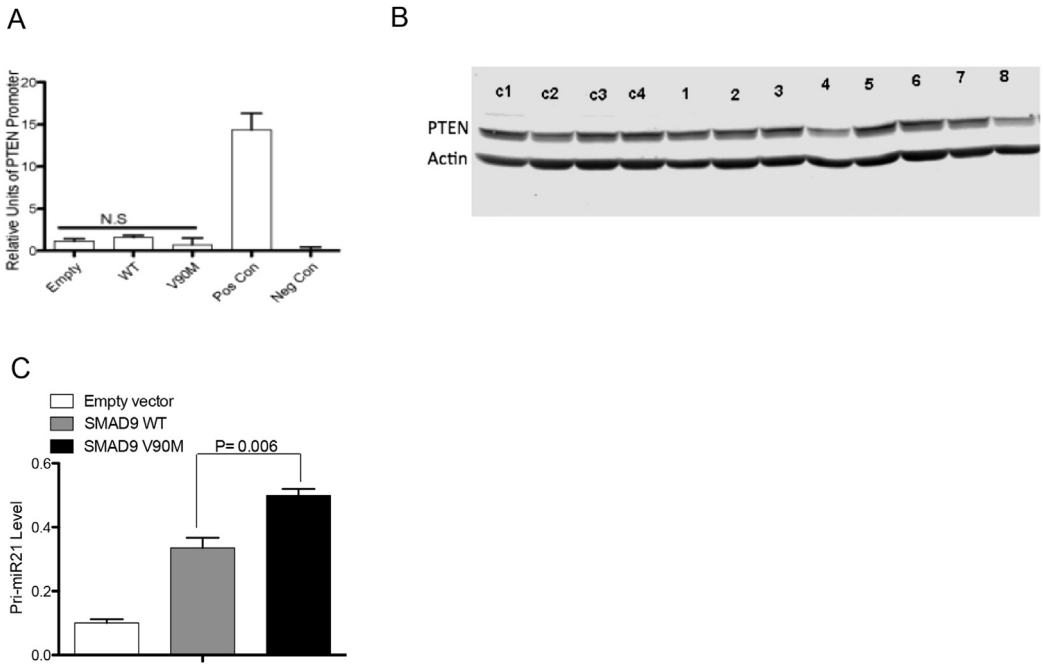

Supplementary Figure 2. (*A*) Immunoblot analysis of PTEN expression in patient-derived lymphoblastoid cells. Immunoblot analysis from lymphoblastoid cell lines was performed using anti-PTEN mouse monoclonal (Cascade Biosciences, Portland, OR) at 1:5000 and anti-ACTIN mouse monoclonal (Santa Cruz Biotechnology, Santa Cruz, CA) at 1:20 000. C1−4 are control research participants, samples 1−4 are from CS patients and samples 5−8 are from HPS patients. PTEN expression was significantly lower in sample 4 (CS patient with germline PTEN deletion) and sample 8, which is our patient 3864TE with the *SMAD9* ^{V90M} mutation. (*B*) No direct binding of SMAD9 with *PTEN* promoter. Chromatin immunoprecipitation (ChIP) analysis was performed on HEK293 cells transfected with empty vector, *SMAD9* ^{WT}, or *SMAD9* ^{V90M} plasmids, respectively, using Flag antibody. ChIP elute was then utilized for quantitative PCR using *PTEN* promoter primers. No significant binding was observed between Flag-SMAD9 and *PTEN* promoter. (*C*) Increased binding between SMAD9 V90M and Pri-miR21 in HEK293 cells. Pri-miR21 reverse transcription PCR was performed from total RNAs extracted from FLAG Immunoprecipitation in HEK293 cells transfected with empty vector, *SMAD9*^{WT} or *SMAD9*^{V90M} vector, respectively. *White bar* represents Pri-miR21 level being pulled down in HEK293 cell transfected with empty vector. *Gray bar* represents Pri-miR21 level being pulled down in HEK293 cell transfected with FLAG tagged *SMAD9*^{WT} vector. *Black bar* represent Pr-miR21 level being pulled down in HEK293 cells transfected with FLAG tagged *SMAD9*^{V90M} vector.

Supplementary Table 1. Characteristics of Heritable Hamartomatous Polyposis Syndromes and Known Involved Signaling Pathways

Polyp histology	Clinical syndrome	Genes suspected	Main canonical pathways affected
Hamartomas/ Juvenile polyps	Juvenile polyposis syndrome	*SMAD4, BMPR1A,*	BMP signaling TGFβ signaling
Hamartomas/ PJ polyps	Peutz-Jeghers syndrome	*STK11 (LKB1)*	AMP-activated protein kinase family
Multiple histologies/ ganglioneuromas	Cowden syndrome	*PTEN, KLLN, SDHx, PIK3CA, AKT1*	PI3K/AKT/MTOR
Ganglioneuromas	MEN 2B	*RET*	GNDF signaling
	NF1 (diffuse)	*NF1*	RAS signaling

AMP, adenosine monophosphate; GNDF, glial cell line–derived neurotrophic factor; MEN 2B, multiple 10 endocrine neoplasia type 2B; MTOR, mammalian target of rapamycin; NF1, type I neurofibromatosis; PI3K, phosphoinositide 3-kinase; PJ, Peutz-Jehgers; TGF, transforming growth factor.